

Statistical application in Image Processing by Integrating C and SAS

Vidhyavathi Venkataraman, Biomarin Pharmaceuticals;
Srinand Ponnathapura Nandakumar, Allogene Therapeutics;
AnupamaDatta, TransUnion

ABSTRACT

Analysis and manipulation of image data after being decoded into a numerical format is known as image processing. Several filters utilizing statistical principles are applied to this numerical data to improve the quality of the image. Beginning with SAS 9.2, a unique procedure is available to incorporate the flexibility of C programs into SAS. In this paper, we discuss the procedure of customizing C functions and integrating them in SAS. An illustration of this feature is used in addressing common issues for image analysis like image size standardization, magnification and pixel transformation/contrasting. Statistical tools like weighted regression (bi-linear interpolation), Expectation Maximization (EM) algorithm in the Region of Interest (RoI) and the Histogram Equalization techniques are detailed for further image enhancement.

INTRODUCTION

Full field digital mammography (FFDM) systems are devices intended for the screening and diagnosis of breast cancer (FDA, 2008). These FFDM systems produce full field digital x-ray images of the breast and include digital mammography software, a full field digital image receptor, an acquisition workstation and signal analysis programs. Gains in the overall diagnostic accuracy of digital mammography as opposed to the film mammography (Yamada, 2010) have made digital mammography an industry standard.

Another field where diagnosis is assisted by imaging is Magnetic Resonance Imaging (MRI). MRI is generally performed to identify tumors, internal bleeding/injury, blood vessel diseases or infection. MRI may also be used to provide more information about a problem seen on an X-ray, ultrasound scan, or a Computed Tomography (CT) scan. Contrasting these MRI images can show abnormal tissues more clearly.

Recently, the U.S. Food and Drug Administration (FDA) initiated a re-classification of these systems to class II. Although quality assurance considerations apply to digital imaging, image presentation and standardization are undetermined (Pisano, et al., 2005). The combination of digital mammography acquisition (Cole, et al., 2005) and display systems can lead to clinically significant over or underestimation of lesion size in magnification mode (Paquetel & Hendrick, 2010). We broadly classify the issues during diagnosis using digital images into:

1. Discrepancy between the systems in pixel size (resolution) at acquisition and variable interpretations of the DICOM (Digital Imaging and Communications in Medicine) standards.
2. Disparity between systems when the display images are different from the actual physical size.
3. Discrepancy from different orientation of the images due to proprietary development of products (Pisano, Zuley, Baum, & Marques, 2007)

Despite these concerns, digital imaging is an invaluable tool for diagnostics. In (Acharya & Ray, 2005) several important applications of image processing in field of biomedical Image Interpretation are justified. To alleviate the above mentioned concerns, image processing algorithms were developed to assist in making an informed decision during medical review.

Enhancement of an image involves bringing out detail that is obscured/highlight certain features of interest (Gonzalez & Woods, 2007). There are several software including MATLAB, R, etc which have inbuilt functionality for image processing. One such software capable of image processing is a C language compiler. The C source code, when converted to dynamic libraries (*.dll), is easy to integrate with any of the C compatible languages like SAS.

SAS users have always depended on the macro facility to create and customize user defined functions in the DATA step. However, with the introduction of version 9.2, SAS added the ability to create user-defined functions and call subroutines using the SAS DATA step (Wang & Zhang, 2011). Eberhardt explains with examples the steps involved in incorporating functions created in C using PROC PROTO and PROC FCMP in (Eberhardt, 2009) and (Eberhardt, 2010). PROC PROTO allows the user to register the external functions onto SAS in batch mode using a load module, like dynamic library which contains the compiled C functions (Secosky, 2007). PROC FCMP is used to create 'wrapper' functions which declare the external C functions for SAS to call it in the DATA step. In this paper, we utilize this feature of C and SAS to address some of the concerns regarding digital imaging by analyzing a mammogram and an MRI.

TECHNICAL SPECIFICATION

The source code of C and SAS programs along with the dll files for compilation in the 32/64-bit operating systems and their library settings for reading images are catalogued in GitHub url: <https://github.com/vidhyavathiv/PharmaSUG2019>

There are various graphics file formats available to create and store images, such as *.bmp, *.jpeg, *.gif, etc. In this paper, we restrict our discussion to uncompressed bitmap images and illustrate pixel manipulation for image enhancement using C and SAS. ImageManipulation.dll is a C library with two interfaces:

1. WritePixelsToFile: This C function takes two inputs:
 - a. Path of the source image from which the pixel values are read.
 - b. Path of the file (format being .csv or .txt) to which the pixel values are written to for further calibrations. This function returns 0 on successful execution and -1 on error.
2. createBMPFromFloat: This C function takes three inputs:
 - a. Path of the source image from which the image header information is obtained for creating a new image file.
 - b. Path of the text/csv file which would have the pixel values required to frame a new image.
 - c. Name of the new bitmap file to be created.

The above mentioned functions use an auxiliary function called getImageData for reading the header information of the image. To read the image, we first read the header information (54 bytes) and then the image bytes (3 for each pixel) into an array of size imageHeight x imageWidth. Each RGB byte is stored as an unsigned number in the range of 0-255(Bourke, 1993).

If the image width is not a multiple of 4, image may also have some padding byte which needs to be accounted for, along with the pixel RGB data (Gunawardena, 2011)(Nguyen, 2005). This is because the number of bytes per row of a bitmap file is always grouped into 4 byte blocks. In this paper, we limit our examples to gray scale images where each RGB pixel will have the same pixel intensity. A snippet of the C source code (DreamInCodeForum, 2009) along with the commands to create the library is provided in ImageManipulation.c.

In order to integrate the above C functions in SAS, they are converted to SAS understandable routines. This is achieved with the assistance of PROC PROTO and PROC FCMP. The SAS procedures used to declare and define the compiled C functions (intWritePixelsToFile (), void createBMPFromFloat ()) are explained using three macros in PROTO_FCMP.sas file.

1. %proto_fcmp (dll_folder, output folder) - There are two parameters passed into this macro:
 - a. dll folder - defines the path where ImageManipulation.dll is stored.
 - b. Output folder - defines the library where the PROTO and FCMP datasets that are created during initialization are stored.
2. %getImage(folder, SourceImage, CSVOutput) and %outImage(folder, SourceImage, TextInput, FinalOutput) - The arguments passed through these macros are explained as follows:
 - a. Folder - points to the library where the PROTO and FCMP datasets are stored.

- b. SourceImage and FinalOutput - Path and name of the source bmp and output bmp files respectively.
- c. CSVOutput - Path and name of the csv/text file where the gray scale values of the pixels are written into, from the 'SourceImage' image file.
- d. TextInput - Path and name of the csv/text file where the values of the matrix are read. This file is used to create 'FinalOutput' bitmap.

The initialization process involves calling the compiled dll file (ImageManipulation.dll) from its stored location (dll folder) using LINK command. The two functions, WritePixelsToFile and createBMPFromFloat contained in the dll file are then declared in PROC PROTO package step. The arguments passed through the functions have a return type that is SAS compatible (e.g., char *). The IOTYPE option is used to define all parameters as input to ensure that they will be 'read-only'. The PROTO dataset that is created in this step stores the function prototypes in a user-defined location (output folder).

PROC FCMP is then used to translate WritePixelsToFile () and createBMPFromFloat () into SAS understandable functions sas_bmp2csv () and sas_txt2bmp () respectively. In this step, the wrapper functions are declared using function/subroutine statements. The data type of arguments passed through these functions are also converted to SAS data-step syntax (\$ for char). The INLIB and OUTLIB options allows SAS to call and check the validity of prototypes which are shared between FCMP and PROTO packages. An FCMP dataset is then created at a user determined library (output folder) which stores the information of the wrapper functions.

To store the gray scale values of an image into a csv/txt file, we call sas_bmp2csv () in a data step. A return value of 0 shows that the pixel values of the image was successfully obtained. The path of the image and csv files are determined by the SourceImage and CSVOutput parameters passed through %getImage macro. The sas_txt2bmp () subroutine is used to create a bitmap file from a matrix of unsigned numbers stored in a csv/txt file. The header information required to create this output file is obtained from the source image. Hence, the parameters passed into %outImage () to create the bmp file are SourceImage, TextInput and FinalOutput. Each file path passed into these macros, are followed with \$ sign to indicate to the C compiler that the string has concluded. Option CMPLIB is used in both macros to call for the already compiled FCMP and PROTO datasets stored in user defined locations (folder).

ANALYZING MAMMOGRAM

Digital mammography has been an invaluable tool (Cole, et al., 2005) in breast cancer early detection and diagnosis (Pisano, Zuley, Baum, & Marques, 2007). The National Cancer Institute funded the International Digital Mammography Development Group in the early 90's identifying the importance of digital mammograms. The full list of the FFDM approved by FDA can be found in the FDA website (CDER, 2011). Currently, most manufacturers offer no choice in image processing and change their imaging algorithms from time to time. These changes can significantly alter the appearance of the DICOM which necessitates standardization.

MAGNIFICATION ENHANCEMENT

It is well documented that magnification views can help decrease the number of biopsies performed for suspicious small areas on mammograms (Madan, Nguyen, Wakabayashi , & Beech , 2001).In this section, we address the issue of loss of resolution during magnification of the image. This magnification context can be readily extended to standardize the image size and the pixel count. Consider the example of the mammogram as a grey scale image shown in Figure 1 sourced from (Mammography, 2013).

The C program ImageManipulation.c reads-in this image as continuous values into a matrix. Let's assume that the interest lies in magnifying the suspicious cyst seen in the mammogram. Once this mammogram is read into SAS (refer Mammogram_magnify.sas), we identify the Region of Interest (ROI) with a boundary.

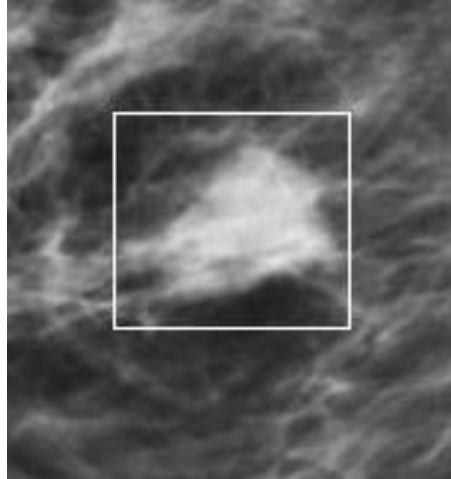


Figure 1: Mammogram region of interest.

A very simple magnification would reproduce the pixel count at each cell within the boundary. If our interest lies in zooming the image five times, it would translate into converting a [2x2] pixel to a [6x6] pixel. We consider two approaches where the ROI is magnified to the size of the original image. In the first approach, the missing cells thus added, are imputed with the original pixel resolution. For the second case, we apply the imputation of bilinear interpolation. Bilinear Interpolation is a re-sampling method that uses the distance weighted average of the four nearest pixel values to impute missing pixels. The enhancement of a [2x2] pixel, as an example using the same pixel density and bilinear interpolation is shown in Table 1.

$$\begin{bmatrix} 0.486 & 0.518 \\ 0.514 & 0.529 \end{bmatrix}$$

The resulting image quality is readily compared in Figure 2. In Figure 2(a), since each pixel is reproduced to a 5x5 matrix, the result is a highly pixilated image which is not very informative. In Figure 2(b), since we applied bilinear interpolation, there is a smooth (weighted) transition between the neighboring cells which leads to a sharper image. The SAS code for both these magnifications is provided in Mammogram_magnify.sas.

$\begin{bmatrix} 0:486 & 0:486 & 0:486 & 0:486 & 0:486 & 0:518 \\ 0:486 & 0:486 & 0:486 & 0:486 & 0:486 & 0:518 \\ 0:486 & 0:486 & 0:486 & 0:486 & 0:486 & 0:518 \\ 0:486 & 0:486 & 0:486 & 0:486 & 0:486 & 0:518 \\ 0:486 & 0:486 & 0:486 & 0:486 & 0:486 & 0:518 \\ 0:514 & 0:514 & 0:514 & 0:514 & 0:514 & 0:529 \end{bmatrix}$	$\begin{bmatrix} 0:486 & 0:493 & 0:499 & 0:505 & 0:511 & 0:518 \\ 0:492 & 0:497 & 0:503 & 0:509 & 0:514 & 0:520 \\ 0:497 & 0:502 & 0:507 & 0:512 & 0:517 & 0:522 \\ 0:503 & 0:507 & 0:512 & 0:516 & 0:520 & 0:525 \\ 0:508 & 0:512 & 0:516 & 0:520 & 0:523 & 0:527 \\ 0:514 & 0:517 & 0:520 & 0:523 & 0:526 & 0:529 \end{bmatrix}$
--	--

Table 1: Applying pixel magnification and bilinear interpolation.

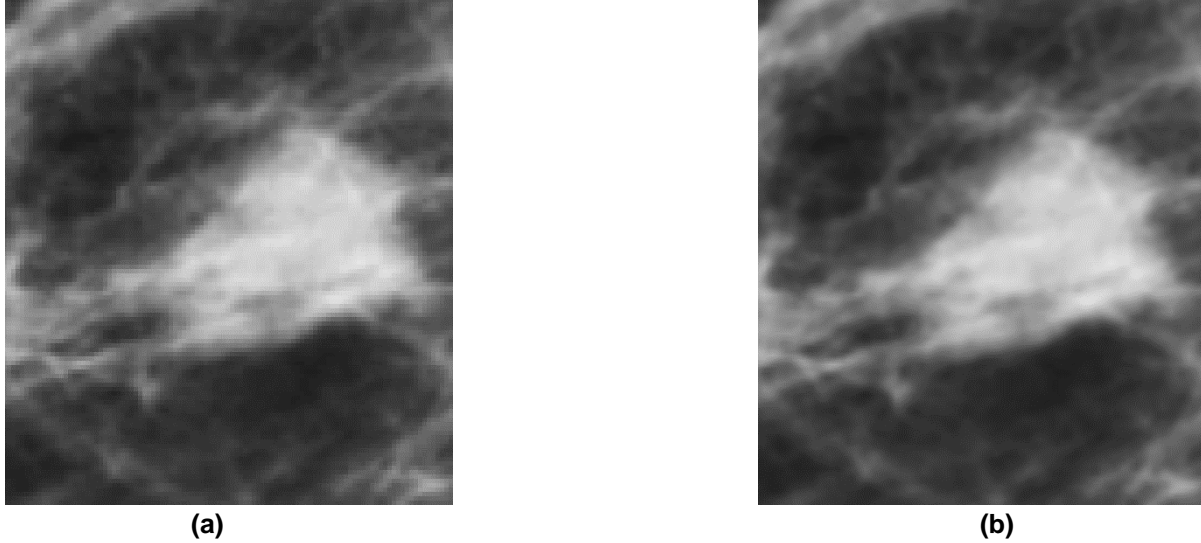


Figure 2: Comparing magnifying versus bilinear interpolation on mammogram ROI.

EM ALGORITHM ON MAMMOGRAM IMAGES

The EM algorithm is an iterative algorithm for parameter estimation by maximum likelihood when some of the random variables involved are not observed/ missing. The term EM was coined in (Dempster, Laird, & Rubin, 1977) where the proof of the algorithm is outlined. With reference to image processing, one can consider the corrupt pixels as missing data and impute using the framework of EM algorithm. EM algorithm in image processing was implemented to estimate the unknown parameters from the observed mammogram in the paper by (Comer, Sheng, & Delph, 1996). These algorithms were also extended on image segmentation after wavelet analysis by (Chen & Lee, 1997). In the paper (Yamazaki, 1998), a color image was treated as a mixture of multi-variate normal from which EM algorithm estimated and improved the parameters of the mixture of densities recursively. In our example, we discuss the brief theory of EM algorithm and apply it to a rectangular section of white pixels.

Consider a random vector y with a known density $f(y, \theta)$ for $\theta \in \Theta$. Based on the Maximum Likelihood (MLE) theory, the log-likelihood of y is defined in Equation (1).

$$l(y, \theta) = \text{LN} L(y, \theta) = \text{LN} \Pi f(y, \theta) \quad (1)$$

By assuming that the data is missing at random (MAR) in the vector y ($y_{\text{observed}}, y_{\text{missing}}$), the revised likelihood function (Dempster, Laird, & Rubin, 1977) in Equation (2) is obtained.

$$l(y, \theta) = l(y_{\text{observed}}, \theta) + l(y_{\text{missing}} | y_{\text{observed}}, \theta) \quad (2)$$

In Mammogram (Figure 3(a)), we identify this missing data by the white rectangular segment. Since white pixels carry an intensity of 1, we reset the white pixel intensity to missing. A window misplaced around this segment identifying the ROI. The steps involved in the EM processes are:

1. E step: Given a set of parameter estimates, such as a mean vector and covariance matrix for a multivariate normal distribution, the E-step calculates the conditional expectation of the complete data log likelihood given the observed data and the parameter estimates i.e., $E_{\theta(t)} = \{l(\theta, y) | y_{\text{observed}}\}$.
2. M step: Given complete-data log likelihood, the M-step finds the parameter estimates to maximize the complete-data log likelihood from the E-step.

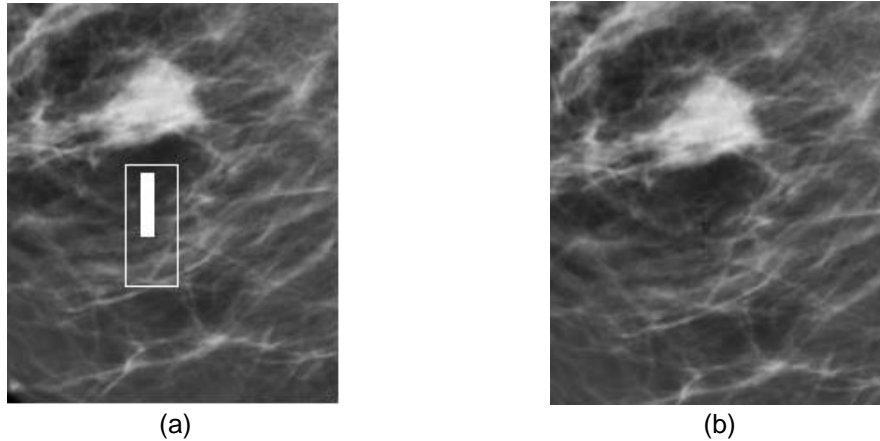


Figure 3: Comparing mammogram before and after EM algorithm.

In SAS (Inc, 2001), these two steps are iterated until the iterations converge i.e., until the difference $l(y, \theta_{t+1}) - l(y, \theta) < \delta$ where δ is a prescribed small quantity. The SAS code Mammogram_EM.sas executes this EM algorithm. Based on the assumption of MAR, the missing pixels get imputed with pixel intensity within the ROI and the resultant Mammogram (Figure 3(b)) is obtained. This application of image processing using EM algorithm within a ROI is called 'Window-Based Image Processing Technique' (Fathy & Siyal, 1998). From this EM application, these missing pixels are imputed with pixel density re-sampled within the ROI.

ANALYZING MRI

In clinical trials, especially in phase II, neuro-imaging is used as a critical end point. This is because radiographic response, in combination with clinical status, is used to assess the therapeutic effect (Hensen , Ulmer , & Harris , 2008). There are two distinct approaches available for the evaluation of contrast-enhancing tumor size on serial imaging studies during clinical trials

1. The diameter-based measurement on a single-axial section containing the largest diameter of tumor, and
2. Computer-assisted volumetric analysis of all sections containing tumor.

Phase II studies are usually conducted in patients with progressive tumors, and serial imaging examinations such as CT scan or Magnetic Resonance Imaging (MRI) are collected after initiation of treatment and compared with a baseline (pre-treatment) profile. Radiographic response for each patient is then assigned according to the grading scale. Some of these include Glioma Grading Scale (GGS), the International Classification of Diseases for Oncology (ICD-O), Kernohan Grading Scale and the St Anne-Mayo Grading Scale.

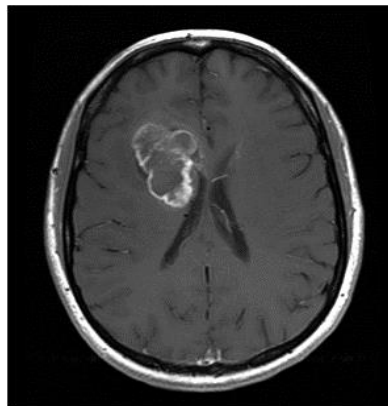


Figure 4: Case study of an MRI

Consider the image of a tumor in Figure 4 sourced from The Cancer Imaging Archive (Purdy , 2011). For this example, we use a grey scale image but, the principle can be extended to any colored image. This is achieved by applying analysis filters separately to the Red, Green and Blue components of the RGB values of the image. The same method on the RGB image may yield dramatic changes in the image's color balance since the relative distributions of the color channels change as a result of applying the algorithm (Naik & Murthy, 2003). A tumor (also called a neoplasm or lesion) is the abnormal tissue that grows by uncontrolled cell division. In this example, the tumor is identified by the milky white profile whose dimension is of interest. The size, i.e., the diameter of the tumor over the period of the drug administration needs to be recorded accurately. Since the pixel intensity ranges from 0 to the maximum intensity, it is standardized to between 0 and 1 (i.e., dividing the intensity with the maximum intensity). From this data, the moments of intensity, such as, the measure of location and spread are presented in Table 2.

Number of data points: 300 columns × 336 rows	= 100800 observations
Mean	= 0.2009
Median	= 0.2118
Std. Deviation	= 0.22403
Inter-quartile Range	= 0.30196

Table 2: Moments of raw pixel intensity from MRI

A greater interest lies in the probability density function of the vector of intensity of this image. From this vector of intensity, a cumulative density function is obtained as shown in Figure 5.

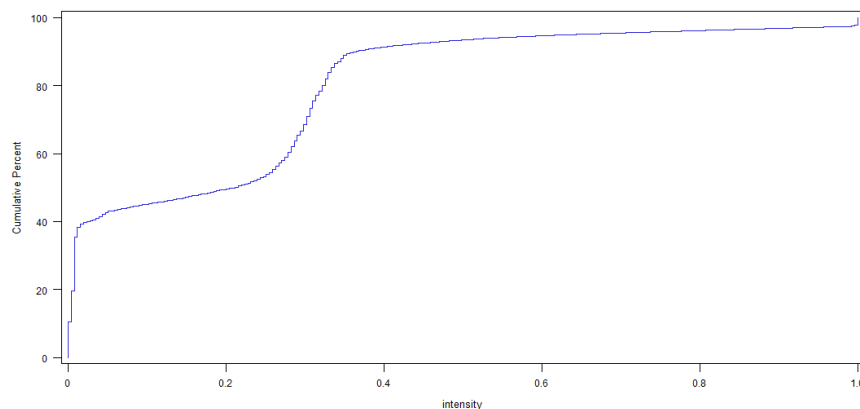


Figure 5: Cdf of the MRI.

LINEAR TRANSFORMATION OF INTENSITY

Let's consider the 'Histogram Equalization Technique' applied to this grayscale image. This is achieved by equating the cumulative density functions (Cdfs) of the old intensity to the new intensity after transformation as seen in the below equations

$$F_{old} (intensity) = G_{new} \{transformed (intensity)\} \quad (3)$$

The probability density function (Pdf) which is the derivative of the old intensity's Cdf can be calculated as shown in the below equation.

$$f_{old} (intensity) = \int_0^{transformed (intensity)} g_{new}(x)dx \quad (4)$$

In this transformed intensity, the normalized histogram is a set to a constant i.e., the pdf of the new image is set to a constant (Donald & Timothy, 1994). For convenience, this constant can be the maximum intensity i.e. $g_{new}(intensity) = 1/\max (intensity)$. In this example, linear transformation is applied across the entire image as opposed to optimizing a segment as in the mammogram example. A simple rearrangement of Equation (4) results in the below transformation

$$\text{Transformed (intensity)} = \text{Max(Intensity)} \times F_{old}(\text{intensity}) \quad (5)$$

With this transformation, the moments from the vector of revised intensity, i.e., the measures of location and spread are computed in Table 3. For this vector of linear intensity, a cumulative density function of new intensity is shown in Figure 6.

Number of data points: 300 columns × 336 rows	= 100800 observations
Mean	= 0.5259
Median	= 0.5017
Std. Deviation	= 0.26757
Interquartile Range	= 00.40104

Table 3: Moments of the standardized pixel intensity from MRI.

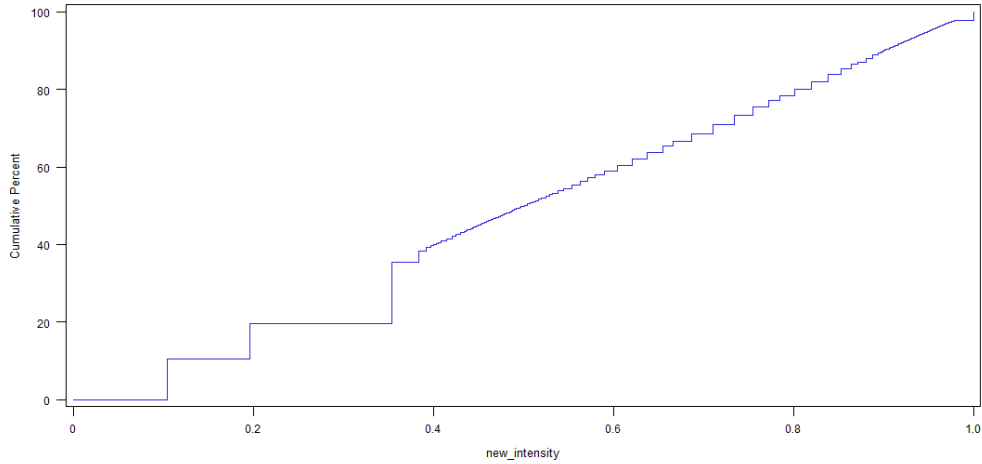


Figure 6: Cdf of the MRI after linear transformation.

Based on the linear intensity, we now reproduce the MRI image of the tumor in Figure 7(a). From this image, several grooves are much clearer. The image can be further sharpened and altered to different views using transformations such as the sine, log, etc. In the next section, we present a technique to enhance the profile of the tumor using the pixel based transformation with power law.

PIXEL BASED TRANSFORMATION

A pixel based transformation (Equation (6)) may be more applicable in this scenario to depress or improve the contrast to obtain a clear profile of the tumor. In this example, the low intensity can be depressed to smaller value while the higher intensity can be improved to even higher values (Schulz , 2012). To setup such a transformation, a mathematical equation (Solomon & Breckon, 2011) is developed using Power Law (Misra, Desai, Hayder , & Karande, 2008). There are several functions which can produce such results. One such equation is shown below

$$\text{Intensity}_{\text{new}} = \begin{cases} \frac{1}{2} \left(\frac{\text{Intensity}_{\text{old}}}{1/2} \right)^\alpha & \dots 0 \leq \text{Intensity}_{\text{old}} \leq t \\ 1 - \frac{1}{2} \left(\frac{\text{Intensity}_{\text{old}}}{1/2} \right)^\alpha & \dots t \leq \text{Intensity}_{\text{old}} \leq 1 \end{cases} \quad (6)$$

Thresholding is a point-based operation that assigns the value between 0 and 1 to each pixel of an image based on a comparison with some global threshold value t (WLS, 2013). Alpha (α) is an amplification value. For α greater than 1, the grey scale image intensity with a lower values ($<t$) get deflated closer to zero and the higher grey scale values ($\geq t$) get inflated to 1. There are several adaptive rules to set α and t values (Schulz , 2012)(Arici & Altunbasak , 2006) . In our example, we set the threshold (t) at 0.5 and the amplification level of 5. From the revised intensity, the new image in Figure 7(b) is generated (refer Tumor.sas). On comparing the original and revised images, we see that the profile of the tumor is much

clearer after the transformation. This enhancement of the boundary of the tumor would greatly assist in estimating the measure of the largest diameter. Besides the above example, several adaptive techniques (Moussa, Aimar-Beurton, & Desbarats, 2011) can readily be applied to these images to explore additional information.



Figure 7: Comparison of the linear and pixel transformed MRI.

DISCUSSION

One of the common issues in diagnosis using an MRI is assessment of the tumor size. A benign brain tumor grows slowly, has distinct boundaries and rarely spreads. However, a malignant brain tumor grows quickly, has irregular boundaries and spreads to nearby brain areas. From Figure 7 (b), the tumor area can be calculated by the number of pixels within the circumference as calculated in `Tumor_ratio.sas`. For this image, the area or pixel count within the tumor was 2459 pixels. In patients undergoing medication, the baseline and post-treatment MRI can be compared to determine treatment efficacy. For instances where the sizes of the images vary, two solutions can be considered:

1. The two images can be resized (as explained in the Mammogram section) to the same pixel count (akin to least common multiple) to compare the two images or
2. A tumor to brain pixel count can be computed to check if the tumor increased in size relative to the brain size. In the above example (Figure 7(b)), this ratio of the pixel counts is 4.304% (ratio of 2459/57133).

Besides brain tumor, imaging is also used for the diagnosis of other tumors. Imaging response guidelines called Response Evaluation Criteria In Solid Tumors (RECIST) were published in 2000. This new criteria was designed as a uniform, simplified, and conservative standard to determine response to therapy for solid tumors. RECIST has not been widely adopted for clinical trials involving brain tumors (Therasse, et al., 2000) however, a majority of the clinical trials evaluating cancer treatments for objective response in solid tumors are using RECIST (FDA-CDER, 2006). This paper assists in profiling the tumor using which the RECIST criteria can be used to categorize into the set of published rules that define when cancer patients improve ("respond"), stay the same ("stabilize"), or worsen ("progression") during treatment.

CONCLUSION

In this paper, we have implemented image processing by integrating C and SAS. For this, we explored the FCMP procedure from SAS to integrate C programs for converting the grey scale image to a data matrix. A simple extension of these programs can be used for RGB colored image analysis. With examples on Mammogram and MRI, we have addressed common issues of standardization of image size, magnification and pixel transformation/contrasting. From these examples, we see the extensibility and further scope to implement the readily available statistical packages in SAS such as Wavelet analysis

(Lane, 2012) to further image enhancement. Since SAS is a validated tool for statistical analysis in the clinical industry, this paper is a natural extension for medical image analysis.

REFERENCES

- Acharya , T., & Ray, A. K. (2005). *Image Processing: Principles and Applications*. John Wiley & Sons.
- Arici , T., & Altunbasak , Y. (2006). Image Local Contrast Enhancement Using Adaptive Non-Linear Filters. *IEEE International Conference on Image Processing* , 2881-2884.
- Bourke, P. (1993). *A Beginners Guide to Bitmaps - Renderings and models by Peter Diprose and Bill Rattenbury*A *Beginners Guide to Bitmaps*.
- CDER, F. (2011). *Radiation-Emitting Products*.
- Chen, C. H., & Lee, G. G. (1997). Image segmentation using multiresolution wavelet analysis and expectation-maximization (EM) algorithm for digital mammography. *International Journal of Imaging Systems and Technology* , 8 (5), 491-504.
- Cole, E., Pisano , E., Zeng , D., Muller , K., Aylward , S., Park , S., et al. (2005). The effects of gray scale image processing on digital mammography interpretation performance. *Academic Radiology* , 12 (5), 585-95.
- Comer, M. L., Sheng, L., & Delph, E. J. (1996). Statistical Segmentation of Mammograms. *Proceedings of the 3rd International Workshop on Digital Mammograph*.
- Dempster, A., Laird , N., & Rubin , D. (1977). Maximum Likelihood From Incomplete Data Via the EM Algorithm. *Journal of the Royal Statistical Society* , 39, 1-38.
- Dempster, A., Laird, N., & Rubin, D. (1977). Maximum Likelihood From Incomplete Data Via the EM Algorithm. *Journal of the Royal Statistical Society Series B (Methodological)* , 39 (1), 1-38.
- Donald, S. L., & Timothy, S. J. (1994). Image Reconstruction and Restoration. *The International Society for Optical Engineering (SPIE)*, 2302.
- DreamInCodeForum*. (2009). Retrieved from </dream.in.code>: //www.dreamincode.net/forums/topic/147643-read-bmp-pixel-by-pixel/
- Eberhardt , P. (2010). Functioning at an Advanced Level PROC FCMP and PROC PROTO. *SAS Global Forum* .
- Eberhardt, P. (2009). A Cup of Coffee and Proc FCMP: I Cannot Function Without Them. *SAS Global Forum* .
- Fathy, M., & Siyal, M. (1998). A window-based image processing technique for quantitative and qualitative analysis of road traffic parameters. *IEEE Transactions on Vehicular Technology* , 47 (4), 1342 - 1349.
- FDA, I. (2008). *Initiates Reclassification of Full Field Digital Mammography Systems*. *Center for Integration of Medicine and Innovative Technology*.
- FDA-CDER. (2006). *Primary Brain Tumor Endpoints: AACR/FDA Public Workshop on Clinical Trial End Points in Primary Brain Tumors*.
- Gonzalez , R. C., & Woods , R. E. (2007). *Digital Image Processing*. Prentice Hall.
- Gunawardena, A. (2011). *Effective Programming in C and Unix*.
- Hensen , J., Ulmer , S., & Harris , G. (2008). Brain Tumor Imaging in Clinical Trials. *American Journal of Neuroradiology* , 29, 419-424.
- Inc, S. I. (2001). *The MI Procedure*. Cary, NC.
- Lane, M. (2012). An Introduction to Wavelet Analysis with SAS®. *NESUG 18* .
- Madan, A., Nguyen, M., Wakabayashi , M., & Beech , D. (2001). Magnification Views of Mammography Decrease Biopsy Rates. *The American Journal of Surgery* , 67 (7), 687-689.
- Mammography. (2013). Mammography Screening. Retrieved from https://openi.nlm.nih.gov/imgs/512/84/3224926/PMC3224926_1746-1596-4-30-1.png
- Misra, K., Desai, K., Hayder , R., & Karande, S. (2008). Complexity Reduction Using Power-Law Based Scheduling For Exploiting Spatial Correlation in Distributed Video Coding. *15th IEEE International Conference on Image Processing* .

- Moussa, R., Aimar-Beurton, M., & Desbarats, P. (2011). Image Processing on MR Brain Images Using Social Spiders. In *Multi-Agent Systems - Modeling, Control, Programming, Simulations and Applications*.
- Naik, S., & Murthy, C. (2003). Hue-preserving color image enhancement without gamut problem. *IEEE Trans. Image Processing* , 12 (12), 1591 - 1598.
- Nguyen , P. T. (2005). *Bitmap File Format and Manipulation*. Technical report, Osram Opto Semiconductor .
- Paquelet , J., & Hendrick , E. (2010). Lesion Size Inaccuracies in Digital Mammography. *American Journal of Roentgenology* , 194 (1), 115-118.
- Pisano, E. D., Zuley, M., Baum, J. K., & Marques, H. S. (2007). Issues to Consider in Converting to Digital Mammography. *Radiologic clinics of North America* , 45 (5), 813-830.
- Pisano, E., Gatsonis , C., Yale , M., Hendrick , E., Baum , J., Suddhasatta , A., et al. (2005). Diagnostic Performance of Digital Versus Film Mammography For Breast-Cancer Screening. *New England Journal of Medicine* , 353, 1773-1783.
- Purdy , M. (2011). *Online Archive to Link Tumor Scans, Genetic Data*.
- Schulz , T. (2012). *Contrast Transformation By a Pixel Based Intensity Transformation Based on a Simple Power-Law S-Curve*. Contrast Transformation.
- Secosky, J. (2007). User-Written DATA Step Functions. *SAS Global Forum* .
- Solomon, C., & Breckon, T. (2011). *Fundamentals of Digital Image Processing: A Practical Approach with Examples in MATLAB*. Wiley-Blackwell.
- Therasse, P., Arbuck, S. G., Eisenhauer, E. A., Wanders , J., Kaplan , R., Rubinstein , L., et al. (2000). New Guidelines to Evaluate the Response to Treatment in Solid Tumors. *Journal of National Cancer Institute* , 205-216.
- Wang, S., & Zhang, J. (2011). Developing User-Defined Functions in SAS®: A Summary and Comparison. *SAS Global Forum* .
- WLSO, C. (2013). Retrieved from Image Processing:
<http://reference.wolfram.com/mathematica/tutorial/ImageProcessing.html>
- Yamada, T. (2010). Current status and issues of screening digital mammography in Japan. *Breast Cancer* , 17 (3), 163–168.
- Yamazaki , T. (1998). Introduction of EM Algorithm into Color Image Segmentation. In *Proceedings of ICIRS*.

CONTACT INFORMATION

Your comments and questions are valued and encouraged. Contact the author at:

Vidhyavathi Venkataraman
 BioMarin Pharmaceuticals
 vidhyavathi.venkataraman@gmail.com